J. Membrane Biol. 134, 213–224 (1993)

The Journal of
Membrane
Biology
© Springer-Verlag New York Inc. 1993

Platelet Activating Factor-Induced Increase in Cytosolic Calcium and Transmembrane Current in Human Macrophages

C. Katnik, D.J. Nelson

The University of Chicago, Dept. of Neurology and the Committee on Cell Physiology, MC 2030, 5841 S. Maryland Ave., Chicago, Illinois 60637

Received: 1 September 1992/Revised: 2 February 1993

Abstract. Platelet-activating factor (PAF) is synthesized and secreted by macrophages in response to inflammatory stimuli. When exogenously applied to human monocyte derived macrophages (HMDMs), PAF induces a rapid rise in cytosolic free calcium (Ca_i) believed to be an early triggering event in macrophage activation. We investigated PAF-induced Ca^{2+} signaling in HMDMs using the calcium indicator Fura-2, combining single cell ratio fluorimetry and digital video imaging with whole-cell recording techniques. Application of PAF (20 ng/ml) to adherent macrophages induced transient increases in Ca_i that were biphasic, consisting of an initial phase that could be observed in Ca^{2+}-free solutions and a second phase that was critically dependent upon Ca^{2+} entry. When Mn^{2+} was applied to cells in the presence and absence of Ca^{2+}, PAF increased the rate of Mn^{2+} entry rate only when Ca^{2+} was absent. PAF increased the rate of Ba^{2+} entry even when measured in the presence of external Ca^{2+}. Ca^{2+} entry was reversibly inhibited in the presence of external La^{3+} (1 mM). Data obtained from simultaneous voltage-clamp/microfluorimetry experiments demonstrated the activation of a nonselective cation current which closely paralleled the rising phase of the Ca_i transient. We investigated whether the nonselective cation conductance provided for the bulk of the agonist-induced Ca^{2+} influx. Changes in Ca_i following removal of extracellular Ca^{2+} (Ca_o) during the agonist-induced Ca_i response were not associated with changes in whole-cell current. The inability to detect whole-cell current changes correlated with a decrease in Ca_o suggests that the bulk of the Ca^{2+} influx was not through the nonselective conductance and either does not occur through a conductance pathway or occurs via a parallel pathway consisting of channels which are both low conductance and highly Ca^{2+} selective.

Key words: Platelet activating factor — Macrophage activation — Secretion — Calcium homeostasis — Fura-2 — Ion channels

Introduction

Macrophages enter an activated state following the interaction of soluble substances, macroscopic particles, or tumor cells with corresponding receptors at the cell surface. Receptor occupancy initiates a complex signal transduction cascade, ultimately resulting in the initiation of a respiratory burst with the concomitant secretion of reactive oxygen intermediates as well as a variety of factors capable of regulating the proliferation and function of other cells. The mechanisms by which ligation of macrophage surface receptors are transduced into intracellular messages appear to involve changes in Ca_i levels, cAMP elevation, protein phosphorylation, and ion channel activation.

Platelet activating factor (PAF) is an alkyl ether-containing phospholipid synthesized and secreted by macrophages in response to inflammatory stimuli (Braquet et al., 1987). PAF can act as an activation stimulus in an autocrine manner when exogenously applied to macrophages. In peritoneal macrophages, PAF stimulates chemotaxis and the accumulation of inositol phosphates and *sn*-1,2-diacylglycerol (DAG) from sources not solely attributable to phosphotidylinositol metabolism via a mechanism which is subsequent to the activation of protein kinase C (Prpic et

Correspondence to: D.J. Nelson

al., 1988; Uhing et al., 1989). PAF binding to specific surface receptors elicits an increase in Ca_i which is generated in part through release of Ca^{2+} from intracellular stores and in part from the influx of Ca^{2+} from the extracellular solution (Conrad & Rink, 1986; Prpic et al., 1988; Randriamampita & Trautmann, 1989). The PAF-receptor from guinea-pig lung has recently been cloned and functionally expressed in *Xenopus* oocytes (Honda et al., 1991). The hydropathy profile of the cloned receptor with seven putative membrane-spanning domains is similar to other cloned G-protein-linked receptors of the rhodopsin superfamily (Dixon et al., 1986). Thus, elucidation of the signal transduction events accompanying PAF-receptor ligation may lead to an understanding of signaling through other related G-protein-linked chemotactic and eicosanoid receptors, e.g., the thromboxane A_2 and C5a receptors which have been recently cloned (Gerard & Gerard, 1991; Hirata et al., 1991) and are expressed on the macrophage plasma membrane.

We have investigated PAF-induced Ca^{2+} signaling in HMDMs using Fura-2 based microfluorimetry and digital imaging, as well as simultaneous whole-cell voltage-clamp/Fura-2 microfluorimetry. The purpose of this study was to examine conductance changes associated with the receptor-mediated Ca^{2+}entry elicited by PAF. In the absence of contaminating outward K^+ current activation, PAF activated a membrane current which was temporally correlated with changes in Ca_i. The agonist-associated current was nonselective and permeant to N-methyl-D-glucamine (NMDG) used as an impermeant cation substitute. Although nonselective current activation showed tight temporal correlation with the onset of the PAF-induced Ca_i transient, reversible decreases in Ca_i following repeated removal of Ca_o during the Ca_i transient were not correlated with changes in whole-cell current. The inability to detect whole-cell current changes correlated with a decrease in Ca_o suggests that the bulk of the agonist-induced Ca^{2+} entry is not through the nonselective cation conductance and either does not occur through a conductance pathway or occurs via a parallel pathway consisting of channels which are both low conductance and highly Ca^{2+} selective.

Materials and Methods

Cell Culture

Mononuclear cells isolated from peripheral blood samples collected from healthy human volunteers were separated from neutrophils and erythrocytes by Ficoll-Hypaque density gradient centrifugation as previously described (Nelson, Jow & Jow, 1990). Cells were maintained in suspension culture and plated on glass-bottom culture dishes approximately 4–8 hr prior to recording. Dishes, which served as recording chambers, were constructed as follows: an 18 mm diameter hole was punched into the bottom of a 35 mm plastic culture dish. A 22 × 22 mm, acid-cleaned coverslip was fixed to the dish outside surface covering the hole, using Sylgard 184 silicone elastomer (Dow-Corning, Midland, MI). Dishes were placed in a drying oven at 55°C for 1 hr to allow for sufficient Sylgard curing and sterilized with 70% ethanol immediately prior to use. A drop of the mononuclear cell suspension (0.5 ml) was placed in the center of the exposed coverslip and incubated for 1 hr at 37°C in a humidified 5% CO_2:95% O_2 environment. Following incubation and initial cell attachment, 1.5 ml of RPMI growth medium supplemented with antibiotics was added to the dish and the cells were incubated for at least an additional hour.

Cell Loading with Fluorescent Probes

Unattached cells were removed prior to loading with Fura-2 acetoxy methyl ester (5 μM) for 1.5 hr at room temperature in RPMI. This loading solution also contained 0.2% pluronic acid to obtain maximum dye dispersion and 0.5% bovine serum albumin (BSA) to prevent nonspecific dye binding. Following the loading procedure, cells were washed and incubated for 30 min with extracellular solution (mM: 140 NaCl, 5.4 KCl, 2 $CaCl_2$, 2 $MgCl_2$, 10 HEPES, pH 7.4) to allow time for maximal dye deesterification. Cells were washed again prior to use. All experiments were performed within 2 hr after completion of Fura-2 loading. Using this optimized loading protocol, we obtained homogenous dye distribution, as visualized using video-imaging techniques, with minimal punctate cytoplasmic accumulations such as have been described by others for the murine peritoneal macrophage and the macrophage-like cell lines J774 and HL-60 (Malgaroli et al., 1987; Steinberg, Newman & Swanson, 1987; Di Virgilio et al., 1988).

Microfluorimetry

Experiments were performed on a Leitz microscope equipped with UV transparent optics. Dye excitation illumination was provided by a Photon Technology International (PTI) D-101 dual wavelength illumination system. The D-101 consisted of a 75 W Xenon arc lamp, a variable speed reflective optical chopper and two monochromators both under computer control. The illumination system was coupled to the microscope via a fiber optic cable that mixes and randomizes the output of the two monochromators over the field of view. Excitation light was deflected with a 450 nm dichroic mirror through either a 40× phase (Nikon Fluor, N.A. 0.85) or 40× oil-immersion (Nikon Fluor, N.N. 1.3) objective. Emitted fluorescence filtered at 510 nm was collected by a Hammamatsu R928 photomultiplier tube and photon-counting photometer through a variable rectangular aperture roughly equal to the area of the single cell. Photomultiplier output was sampled at 20 Hz and processed using a PTI interface on a NEC 386/20 personal computer. The monochromator slit widths were set at 12 nm.

Cells chosen for experiments were loaded to levels which were at least 10 times that measured for a cell-free area of the coverslip using the masking iris set to the size of the cell. Cells in which resting 340/380 ratios were high (presumably due to plasma membrane damage) were excluded from study.

Fluorescence Ratio Imaging

Cells were illuminated using the dual-monochromator, Xenon-light source as described above. In the imaging experiments, a 20× (Nikon Fluor, N.A. 0.75) objective was used to gather fluorescence data from a number of cells in the field of view. Fluorescence emission was collected with a Hammamatsu c2400 SIT video camera connected to a PTI image processor. Individual frames were summed (number of frames summed depended on loading intensity) and averaged. Frame averages acquired at each wavelength were collected at predetermined intervals and stored on hard disk for off-line analysis. Frame averages at each wavelength were divided pixel by pixel to yield ratio images.

Dye Calibration

For the majority of the experiments, changes in Ca_i were expressed only as the ratio (R) of dye fluorescence at 340 and 380 nm. In those experiments which necessitated an estimate of Ca_i, values for R were converted to Ca^{2+} concentration according to the equation:

$$[Ca] = K_D(R - R_{min})/R_{max} - R)(S_{f2}/S_{b2}) \quad (1)$$

where K_D = 327 nM, S_{f2}/s_{b2} = 8.42, R_{min}= 0.333, and R_{max} = 7.41 and where λ_1 = 340 nm and λ_2 = 380 nm were determined from standard solutions of known Ca^{2+} concentration (Grynkiewicz, Poenie & Tsien, 1985).

Electrophysiology

Simultaneous microfluorometric measurements of Ca_i and membrane current were correlated in single cells. Standard whole-cell recordings of membrane current were carried out using methodology previously described (Nelson, Jow & Jow, 1990).

PAF was applied locally to the voltage-clamped cell using a puffer pipette. In some of the studies, a single puffer pipette was used and solutions were changed by accessing different reservoirs. Although this technique had the advantage of localizing solution changes to a single cell, it was impossible to obtain fast exchanges between solutions. Therefore, an alternative superfusion system was developed whereby adjacent puffer pipettes were mounted side by side and positioned near the voltage-clamped cell. Using this modification, changes between solutions were rapidly brought about by starting and stopping flow in a particular pipette. This was especially important when rapid solution exchanges were used to determine the reversibility of current inhibition during a transient Ca_i response. Whole bath exchanges were accomplished using a gravity-fed solution input and a vacuum-aspirated output.

Summary data are expressed as means ± SEM with the number of experiments in parentheses.

Solutions

The standard internal (pipette) solution with 38 nM free Ca^{2+} contained (in mM): 140 KCl, 2 $MgCl_2$, 2 $CaCl_2$, 11 ethylene glycol-bis(β-aminoethyl ether)-N,N,N′,N′-tetraacetic acid (EGTA)-KOH, and 10 N-2-hydroxy-ethylpiperazine-N′-2-ethanesulfonic acid (HEPES); pH 7.2. When $Cs^+$was used in the internal solution, K^+ was replaced with an isosmolar amount of the Cs^+ salt. The bath solution contained (in mM): 140 NaCl, 5.4 KCl, 2 $CaCl_2$, 1 $MgCl_2$, and 10 HEPES; pH 7.4. In those experiments where both K^+ and Na^+ in the external and internal solutions were replaced with the cation N-methyl-D-glucamine (NMDG), the external solution contained (in mM): 140 NMDG-Cl, 2 $CaCl_2$, 2 $MgCl_2$, and 10 HEPES buffered to pH 7.4. The pipette solution contained 40 NMDG-Cl, 100 NMDG-glutamate, 1.0 EGTA, 0.2 $CaCl_2$, 2 $MgCl_2$ and 10 HEPES; pH 7.2. Agar bridges were used for electrical connections to both bath and pipette electrodes to minimize junction potential artifacts in NMDG-glutamate containing solutions. ATP (0.3 mM), GTP (0.3 mM) and GTPγS (0.1 mM) were added to pipette solutions containing 0.1 mM pentapotassium Fura-2 in experiments in which cells were loaded with the dye via the pipette. Solution osmolarities were monitored using a vapor pressure osmometer (Model 5500, Wescor, Logan, UT).

Results

Biphasic Nature of the PAF-Induced Ca_i Transient and Dependence upon External Ca^{2+}

PAF application to HMDMs elicited a transient, biphasic increase in Ca_i (Fig. 1*A* and *B*). Subsequent applications of PAF failed to induce a second Ca_i transient following washing even after a period of 2 hr. Exogenous application of the autocoid produced a rapid increase in Ca_i, which reached peak levels 5–10 times that measured at rest followed by a slower, sustained elevation in Ca_i, which returned to basal levels with a variable time course over a period of minutes. Changes in Ca_i were measured as an increase in the 340/380 fluorescence intensity ratio ($R_{340/380}$). Mean initial, peak, and steady-state $R_{340/380}$ values observed in 41 cells prior to and following PAF stimulation were 0.63 ± 0.04 ($Ca_i \approx$ 50 nM), 1.60 ± 0.15 ($Ca_i \approx$ 415 nM), and 0.90 ± 0.11 ($Ca_i \approx$ 109 nM), respectively. Steady-state $R_{340/380}$ mesurements were taken at 1,000 sec following the peak response. The first phase, the rapid increase in Ca_i, was not dependent on the presence of extracellular Ca^{2+} (Ca_o) (Fig. 1*C*) and was, therefore, taken to result from internal store release. A sustained increase in Ca_i was obtained upon readdition of Ca^{2+} to the bathing solution following the decay of the PAF-induced Ca_i transient. Prolonged exposure of the cell to EGTA-buffered, Ca^{2+}-free solutions (5–10 min) during which depletion of intracellular Ca^{2+} stores would be expected to occur, resulted in loss of the PAF-induced Ca^{2+} transient in the absence of Ca_o (Fig. 1*D*). A large increase in Ca_i was observed upon re-exposure of PAF-stimulated, Ca^{2+}-depleted cells to Ca^{2+}-containing solutions. The large increase in Ca^{2+} upon re-exposure of Ca^{2+}-

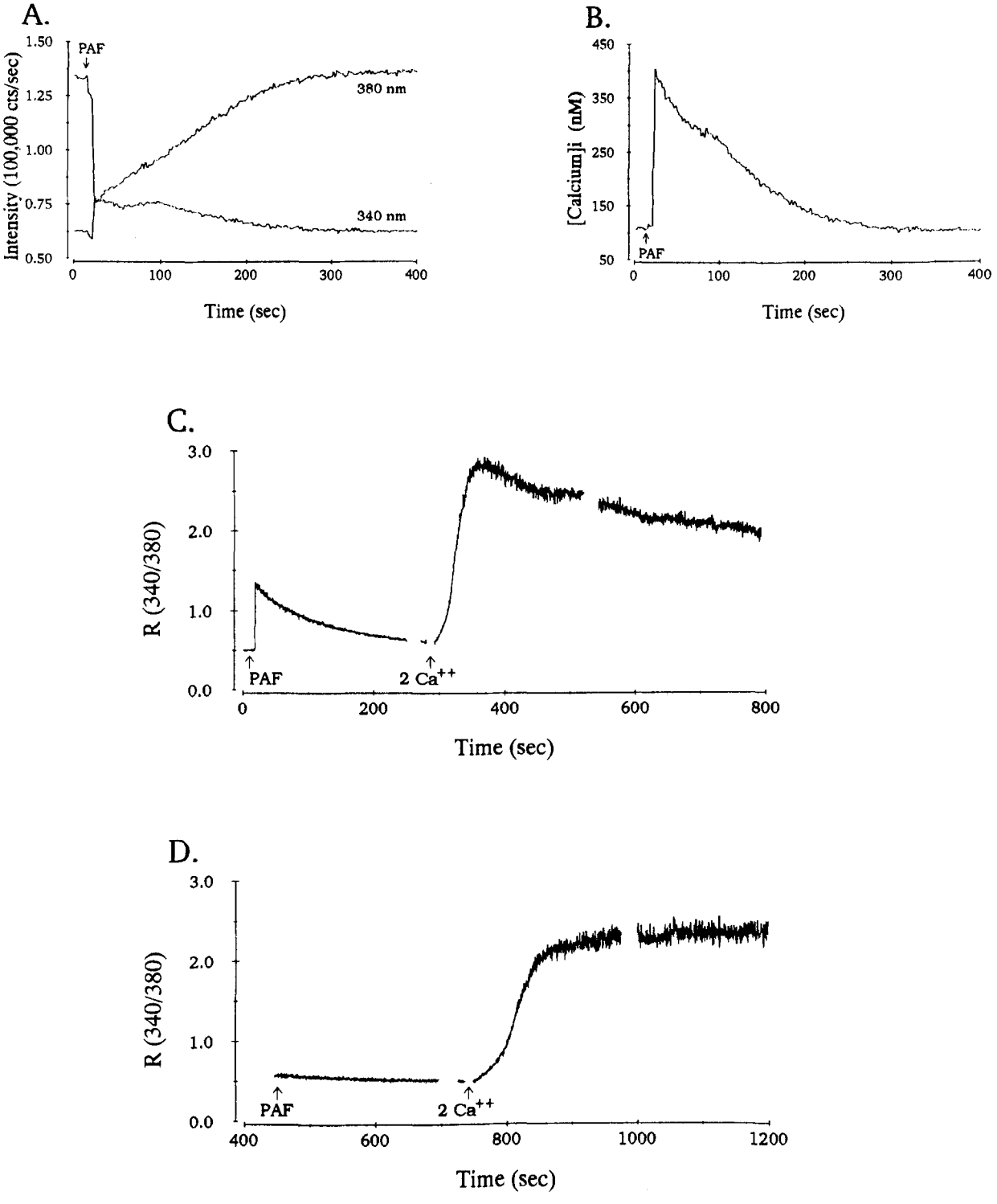

Fig. 1. Dependence of PAF-induced increase in Ca_i in HMDMs on external calcium. (*A*) The change in Fura-2 dye emission at 510 nm following dye excitation at 340 and 380 nm prior to and following exposure of a single cell to PAF (20 ng/ml). Background levels were less than 10,000 cts/sec. (*B*) Calculated changes in Ca_i from the experiment in *A* obtained using Eq. (1). (*C*) Change in Ca_i in response to PAF stimulation in a Ca^{2+}-free solution buffered with 1 mM EGTA. Rapid exchange of a 2 mM Ca^{2+}-containing external solution for a Ca^{2+}-free solution was made approximately 10 sec prior to PAF stimulation. The transient increase in Ca_i is presumably due to Ca^{2+} released from internal stores. Upon readdition of Ca^{2+}-containing external solution, Ca_i increased without delay. (*D*) Equilibration of cells with Ca^{2+}-free external solution for approximately 7 min was used to deplete cells of Ca_i. Stimulation of Ca_i-depleted cells in Ca^{2+}-free solutions eliminated the increase in Ca_i. As seen in *C*, Ca_i increased immediately upon readdition of Ca^{2+}-containing bath solution.

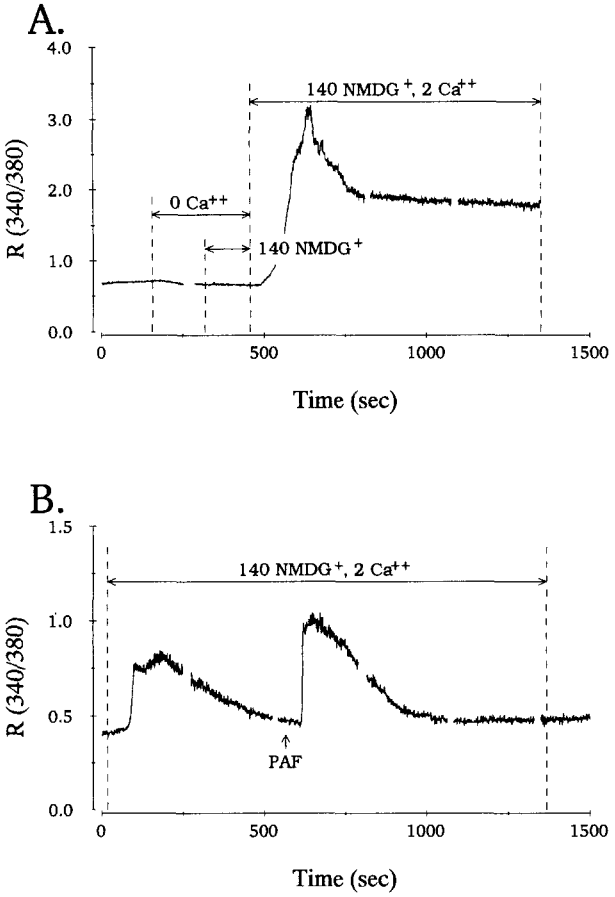

Fig. 2. Contribution of Na-Ca exchange in setting basal Ca_i levels and in determining the decay of the PAF-induced Ca_i transient. (*A*) Changes in Ca_i (expressed as changes in the $R_{340/380}$) following removal of extracellular Ca^{2+}, replacement of extracellular Na^+ with $NMDG^+$ in the absence of Ca^{2+}, and replenishment of extracellular Ca^{2+} in the absence of extracellular Na^+. (*B*) Changes in Ca_i following isotonic substitution of extracellular Na^+ by $NMDG^+$ prior to and following PAF stimulation.

depleted cells to Ca^{2+} was dependent upon the presence of agonist binding. In two experiments in which Ca^{2+}-depleted cells were not pre-treated with PAF, re-exposure to Ca_o did not produce an increase in Ca_i until PAF was applied.

PAF-Induced Ca_i Transients in the Absence of Na-Ca Exchange

Although Na-Ca exchange appears to be important in the maintenance of basal Ca_i levels in HMDMs (Fig. 2*A*), modulation of its activity did not appear to play a role in the PAF-induced increase in Ca_i (Fig. 2*B*). Removal of Ca^{2+} from the external solution led to only a slight decrease in the basal Ca_i level, in the presence or absence of external Na^+ as can be seen in Fig. 2*A*. However, addition of Ca^{2+} to a solution in which external Na^+ (Na_o) was isosmotically replaced with the impermeant cation N-methyl-D-glucamine (NMDG) resulted in an increase in the 340/380 ratio ($R_{340/380}$), which decayed back to a sustained level that varied from cell to cell but which could be significantly elevated over baseline levels, as seen in Fig. 2*A*. In the absence of Na_o, Na-Ca exchanger activity would be expected to be inhibited or reversed depending upon Na_i levels. It should be noted that the magnitude of the increase in Ca_i resulting from the inhibition of Na-Ca exchange was highly variable and was not dependent upon pre-exposure of cells to Ca^{2+}-free solutions. Peak changes in the $R_{340/380}$ measured in 38 cells following removal of Na_o ranged from 0 to 5.2. Following maximal reversal and/or inhibition of Na-Ca exchange, PAF stimulation produced a normal Ca_i transient (Fig. 2*B*). Mean initial, peak, and steady-state $R_{340/380}$ values observed prior to and following PAF stimulation in the absence of Na_o were 0.69 ± 0.02 ($Ca_i \approx 62$ nM), 1.38 ± 0.20 ($Ca_i \approx 282$ nM), and 1.04 ± 0.13 ($Ca_i \approx 149$ nM), respectively. The mean initial, peak, and steady-state $R_{340/380}$ values observed for the PAF-induced Ca_i transients in the presence and absence of Na_o were not significantly different. These results indicate that PAF-induced increases in Ca_i were not due primarily to inhibition of Na-Ca exchange. Additionally, these results demonstrate that the decay of the PAF-induced Ca_i transient was not due to an enhancement of Na-Ca exchange activity although Na-Ca exchange no doubt plays a role in macrophage calcium homeostasis prior to and during a PAF-induced Ca_i transient.

Inhibition of the Sustained Ca_i Phase of the PAF-Induced Ca_i Transient by Polyvalent Cations

The sustained phase of the PAF-induced Ca_i transient was examined in a total of 196 cells in nine separate preparations using fluorescence ratio imaging. The inhibition of receptor-operated Ca^{2+} influx was determined for the polyvalent cation La^{3+}. La^{3+} produced a reversible decrease in Ca_i when added during the initial phase of the PAF-induced Ca_i transient. In one experiment, of the 74 cells which responded to PAF, 63 displayed a reversible La^{3+}-induced decrease in Ca_i (*data not shown*).

Cation Specificity of the PAF-Activated Calcium Influx Pathway

Receptor-operated Ca^{2+} influx pathways permeable to Mn^{2+} have been demonstrated in a number of cell types (Hallam & Rink, 1985; Hallam, Jacob &

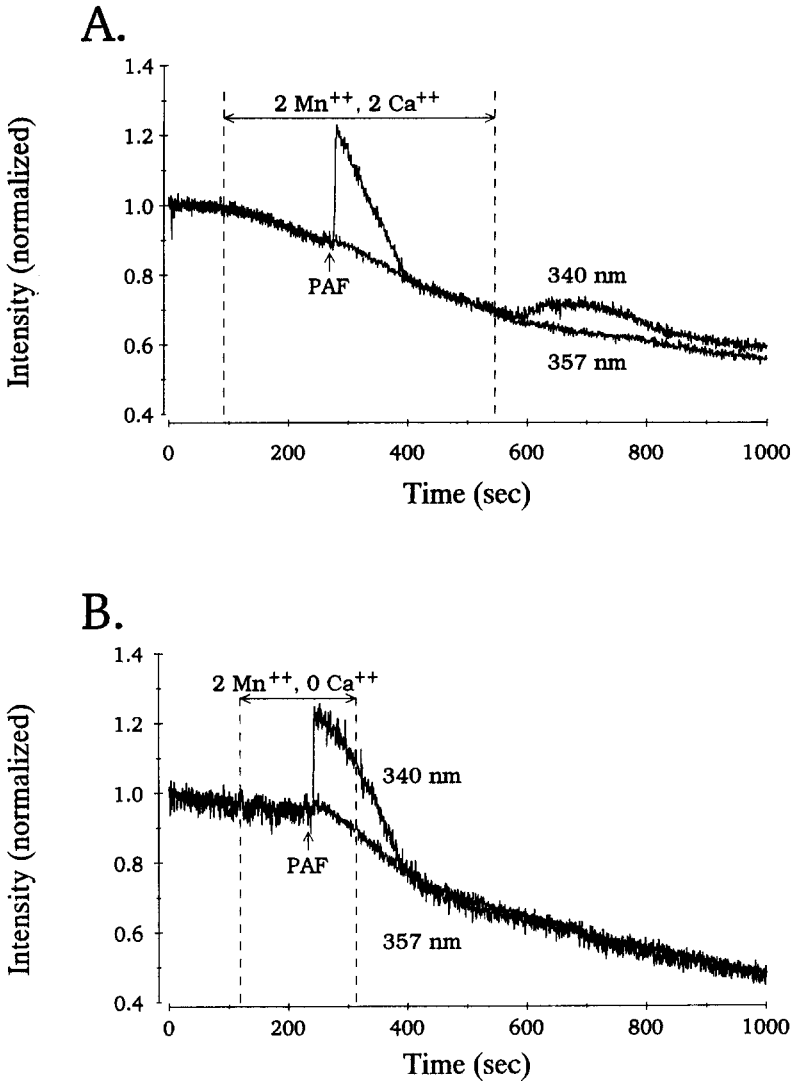

Fig. 3. Temporal correlation between the rapid increase in Ca_i and activation of the Ca^{2+} influx pathway as monitored by Mn^{2+} quench of Fura-2 fluorescence following PAF stimulation. Fura-2 fluorescence was monitored at two excitation wavelengths, 340 and 357 nm (isosbestic wavelength of Ca^{2+}-Fura 2). (*A*) PAF-stimulation of a cell in the presence of external Ca^{2+} (2 mM) and Mn^{2+} (2 mM). PAF stimulation did not appreciably increase Mn^{2+} influx as monitored by changes in the rate of Mn^{2+}-induced dye quenching of the 357 nm signal. (*B*) Stimulation of a cell in the absence of external Ca^{2+} and in the presence of Mn^{2+} (2 mM). Mn^{2+} influx was detectable as an increase in fluorescence quenching following PAF exposure and was temporally correlated with internal Ca^{2+} release as monitored by the Ca^{2+}-sensitive signal (340 nm).

Merritt, 1988; Merritt, Jacob & Hallam, 1989; Kass et al., 1990). It appears that in many cells, Mn^{2+} can enter the cytoplasmic compartment via the same permeation pathway as Ca^{2+} (Jacob, 1990). Since Mn^{2+} binding to Fura-2 quenches the dye's fluorescence, independent of excitation wavelength, the rate of quenching at a Ca^{2+} independent wavelength can be used to measure Mn^{2+} influx while changes in R can be used to measure changes in Ca_i. This provides an estimate of the relative time course of entry pathway activation with respect to the release of Ca^{2+} from stores following agonist stimulation. We monitored Fura-2 fluorescence at the isosbestic point for Ca^{2+} (357 nm) as well as the Ca^{2+}-sensitive wavelength (340 nm). The 340 nm signal allowed us to monitor Ca_i changes and correlate them to the onset of Mn^{2+} entry. Data from a representative set of experiments are given in Fig. 3. Resting cells displayed minimal Mn^{2+}-induced dye quenching (1.2 ± 0.2 percent/min decrease in fluorescence intensity, $n = 10$). With solutions containing Mn^{2+}(2 mM) and Ca^{2+} (2 mM) we were unable to observe an enhancement of Mn^{2+}-induced dye quenching following PAF-stimulation (Fig. 3*A*). Experiments carried out in Ca^{2+}-free solutions containing Mn^{2+}(2 mM) showed a perceptible increase in the dye quench rate following agonist stimulation (5.2 ± 1.2 percent/min, $n= 10$). The Mn^{2+} influx (determined as a rate of change in intensity for the 357 nm signal) lagged the Ca_i increase by 9.7 ± 3.5 sec ($n= 7$). Data in these experiments demonstrate that (i) the influx pathway is impermeable to Mn^{2+}in the presence of stoichiometric Ca^{2+} concentrations, and (ii) there is a temporal delay between the release of $Ca^{2+}$from internal stores and the opening of the divalent entry pathway.

In light of the limited Mn^{2+} permeability of the PAF-stimulated influx pathway, further studies in-

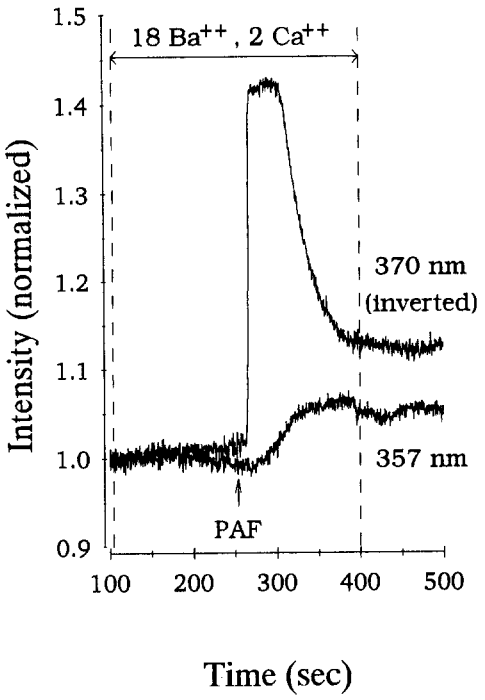

Fig. 4. Temporal correlation between rapid increase in Ca_i and activation of the Ca^{2+} influx pathway as monitored by increases in Ba^{2+}-induced fluorescence following PAF stimulation. The rate of Ba^{2+} entry following PAF stimulation was determined by monitoring the Fura-2 isosbestic point for Ca^{2+} (357 nm). PAF stimulation increased the rate of Ba^{2+} entry, seen as an increase in the fluorescence intensity at 357 nm, almost simultaneously with the PAF-induced increase in Ca_i as monitored by a decrease in the fluorescence intensity on the Ba^{2+}-independent Ca^{2+}-dependent wavelength (370 nm). Note: the Ca^{2+}-dependent wavelength (370 nm) signal which indicates changes in Ca_i is inverted in order to emphasize temporal correlation between the two signals.

vestigating the Ba^{2+}permeability of the entry pathway were performed. Similar experiments have been carried out on receptor-activated Ca^{2+}-influx channels in other preparations (Murray & Kotlikoff, 1991). We examined the Ba^{2+} permeability of the PAF-activated influx pathway by monitoring fluorescence at the Ca^{2+}-dependent wavelength (370 nm, Ba^{2+} isosbestic point) and the Ba^{2+}-dependent wavelength (357 nm, Ca^{2+} isosbestic point). An increase in the 357 nm signal would therefore indicate an increase in the rate of Ba^{2+} entry, while a decrease in the 370 nm signal (which decreases in intensity upon Ca^{2+}binding to the dye) would indicate an increase in Ca_i. Representative results from these experiments can be seen in Fig. 4. In the presence of external Ba^{2+} at a concentration ninefold greater than external Ca^{2+}, we obtained an increase in Ba^{2+} entry following PAF-stimulation. Because the sensitivity of Fura-2 to changes in Ba^{2+} decreases in the presence of Ca^{2+} (we found the apparent K_D of Fura-2 for Ba^{2+} increased by 50% as the free Ca^{2+} concentration increased from 0 to 50 nM yielding values similar to those reported by Kwan and Putney [1990] and Ozaki, Yatomi and Kung [1992]), we were unable to quantitatively assess the magnitude of the Ba^{2+} influx in the presence of changing Ca_i levels. Nonetheless, cells bathed in solutions containing 18 mM $Ba^{2+}$and 2 mM Ca^{2+}showed a 13.3 ± 2.6% increase in fluorescence at 357 nm (n = 6) following PAF stimulation. The Ba^{2+} influx lagged the Ca_i increase by 11.2 ± 2.8 sec, a value not significantly different from the delay in the opening of the divalent pathway measured in the Mn^{2+} quench experiments (9.7 sec, *vide supra*). When the concentration of both Ba^{2+} and Ca^{2+} was 2 mM, there was an 8.0 ± 3.5% increase in fluorescence at 357 nm; however, the rate of change of fluorescence intensity at 357 nm was much more difficult to detect.

Current Activation Associated with the Rising Phase of the PAF-Induced Ca^{2+} Transient

In an attempt to determine the calcium permeability of the inward current associated with the early phase of the PAF-induced Ca_i transient, whole-cell voltage clamp experiments were performed using pipette and bath solutions containing the large cation substitute NMDG as a Na^+ and K^+ replacement, where Ca^{2+} and Cl^- were the major permeant species. Experiments were performed in asymmetrical Cl^- solutions (Nernst potential for Cl^- in these studies was −30 mV), thereby allowing us to identify an increase in the divalent conductance as a depolarizing shift in the zero current potential. Membrane currents were measured in response to 300 msec voltage ramps from −150 to 90 mV applied every 3 sec from a holding potential of −30 mV. Membrane current-voltage (*I-V*) relationships were recorded throughout the PAF-induced Ca_i increase. A prominent inward current was observed at the equilibrium potential for Cl^- following PAF stimulation, consistent with the activation of a cation-selective pathway (Fig. 5*A*). The voltage dependence of the PAF-activated current can be seen in Fig. 5*B*. Current amplitude at a number of hyperpolarized and depolarized potentials prior to and following PAF stimulation was derived from the current recorded during the voltage ramps and plotted as a function of time (Fig. 5*B*). The dependence of the PAF-activated current on Ca_o was examined throughout the response. The Ca^{2+}-containing bathing solution was exchanged repetitively for EGTA-buffered Ca^{2+}-free solutions and the effect on both Ca_i and current examined. Although wide oscilla-

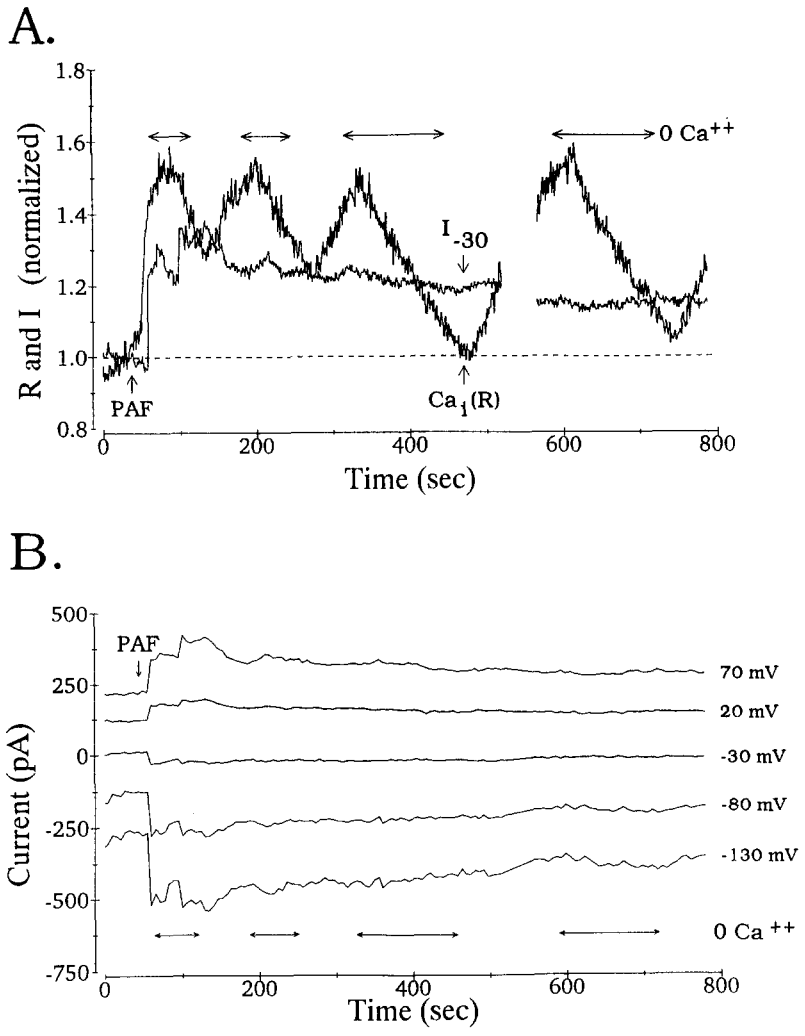

Fig. 5. Calcium permeability of the PAF-activated conductance. Whole-cell currents and Ca_i transient recorded on a cell dialyzed with a pipette solution containing pentapotassium Fura-2 (100 μM). $NMDG^+$ isosmotically replaced Na^+ and K^+ in the bath and pipette solution; glutamate and Cl^- were used as the internal anions. The external bath solution contained (mM) 140 NMDG-Cl and 2 $CaCl_2$ with 10 TEA to block residual outward current. The theoretical equilibrium potential for Cl^- was −30 mV. Holding potential in this experiment was −30 mV; membrane potential was varied from −150 to 90 mV over a 300 msec period every 3 sec as the membrane current was recorded. The bathing solution was periodically exchanged for a Ca^{2+}-free solution buffered with 1 mM EGTA. (*A*) Normalized changes in Ca_i and current at −30 mV (normalized with respect to initial levels, $R_{340/380} = 0.8$, $I_{-30} = -48.1$ pA; current trace is inverted) following PAF stimulation and reversible inhibition of Ca^{++} influx. (*B*) Changes in membrane current at five different potentials obtained from voltage ramps following PAF stimulation and periodic removal of external Ca^{++}.

tions in Ca_i were observed in response to removal of Ca_o, membrane current throughout the potential range showed no obvious dependence upon Ca_o. Current reversal potential at the peak of the PAF-induced Ca_i transient in the presence of Ca^{2+} in the experiment illustrated was −6 mV suggesting that the PAF-activated current was predominantly nonselective. Similar results were obtained in three other cells.

For 21 cells which responded with a transient increase in Ca_i upon PAF stimulation and in which membrane current and Fura-2 microfluorimetry were measured simultaneously in NMDG-Cl bath and pipette solutions, 13 cells responded with an average increase in inward current at −30 mV of 433 ± 93 pA that was associated with the Ca_i transient. Eight cells either failed to respond with current increase or gave a small decrease in current magnitude upon PAF stimulation (average change in current for the nonresponding cells was a decrease in current amplitude of −6.1 ± 3.6). The $R_{340/380}$ in the 21 cells examined increased from a basal level of 0.60 ± 0.03 ($Ca_i \approx 48$ nM) to 1.82 ± 0.23 ($Ca_i \approx 584$ nM) at the peak of the response.

I-V relationships of the PAF-activated current recorded from three representative cells bathed in solutions containing $NMDG^+$ as a Na^+ and K^+ replacement and varying concentrations of Ca_o are illustrated in Fig. 6. Each *I-V* relationship represents the current recorded during a voltage ramp at the peak of the current response minus the current recorded during a ramp prior to PAF stimulation. Even in the presence of elevated Ca_o (20 mM), the PAF-induced current reversal potential indicated the predominant activation of a nonselective conductance through which even a large cation, $NMDG^+$ used as an impermeant cation substitute, is significantly permeant.

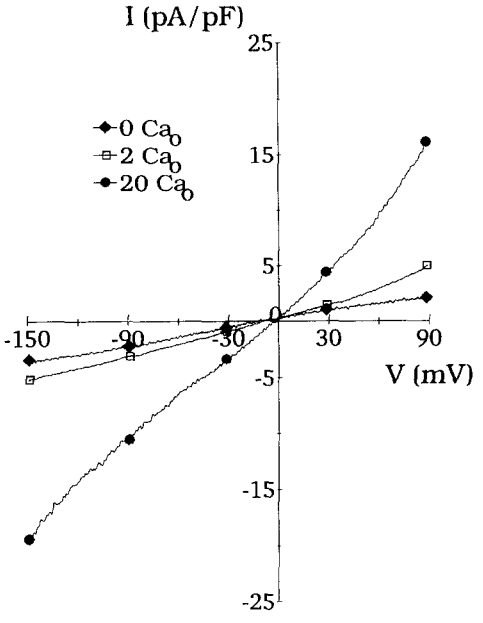

Fig. 6. *I-V* relationship for the PAF-activated current at the peak of the Ca_i transient as a function of external Ca^{2+}. Membrane current was recorded during whole-cell recording, voltage stimuli were delivered and current recorded as in Fig. 5. *I-V* relationship at the peak of a PAF-induced Ca^{2+} transient is shown for three different cells stimulated with PAF in the presence of varying concentrations of Ca_o. Pipette and bath solutions as in Fig. 5; bath solutions contained either 0 Ca^{2+} and 1 mM EGTA (filled diamond), 2 mM Ca^{2+} (open square), or 20 mM Ca^{2+} (filled circle). *I-V* relationships are for PAF-activated current (current at the peak of the Ca_i transient minus current recorded prior to PAF stimulation) normalized to cell capacitance.

Discussion

Data in this study examine the simultaneous measurement of Ca_i and membrane current under voltage clamp in single HMDMs stimulated with PAF. We have confirmed earlier observations made in other macrophage preparations as well as in macrophage cell lines that exogenous PAF produces a transient, biphasic increase in Ca_i composed of an initial rapid increase that declines to a plateau phase which is maintained over a period of minutes. The response is due in part to release of Ca^{2+} from internal stores as well as to influx of Ca^{2+} from surface membranes (Conrad & Rink, 1986; Maudsley & Morris, 1987; Prpic et al., 1988; Ng & Wong, 1989; Randriamampita & Trautmann, 1989, 1990; Randriamampita, Bismuth & Trautmann, 1991; Wood et al., 1991). Electrophysiological characterization of the influx pathway and its temporal correlation with the Ca_i signal has yet to be described in macrophages. Second-messenger-activated nonselective cation current modulated by levels of internal Ca^{2+} has been previously reported in the murine macrophage cell line $P388D_1$ (Lipton, 1986). Randriamampita and colleagues (1991) demonstrated IP_3-induced activation of Ca^{2+}-activated K^+ channels as a direct result of PAF-induced Ca_i rise in murine peritoneal macrophages similar to that induced by α_1-adenoreceptor activation in the same preparation (Hara et al., 1991). Our goal in these studies was to determine (i) the mechanisms behind the transient nature of the PAF-induced Ca_i transient, (ii) the contribution of Ca^{2+} influx during the early phase of the response, and (iii) the temporal relationship between the release of Ca^{2+} from intracellular stores and the opening of the Ca^{2+} influx pathway. Our data are consistent with the conclusion that Ca^{2+} influx is activated with a delay following the initial phase of Ca^{2+} mobilization and that the decay of the response is not due to an enhancement of Na-Ca^{2+} exchange activity. Based on the Mn^{2+} and Ba^{2+}-influx data, the PAF-activated Ca^{2+} influx pathway opens approximately 10–15 sec after the release of Ca^{2+} from intracellular stores. Activation of voltage-independent, nonselective currents was associated with the initial phase of the PAF-induced Ca_i response. However, we were unable to detect changes in whole-cell currents associated with changes in Ca_i observed following repetitive removal of Ca_o during the PAF-induced response, suggesting that the bulk of the influx of Ca^{2+} is either (i) not through a conductance pathway, (ii) a negligible fraction of the total current through a large conductance, nonselective pathway, or (iii) occurs via channels which are both low conductance and highly Ca^{2+} selective.

Dependence of PAF-Induced Ca_i Transient on External Calcium

In the absence of extracellular Ca^{2+}, cells treated with PAF generated a Ca_i transient as a result of internal release. This response was abrogated in calcium-depleted cells exposed for prolonged periods to EGTA. In both cases, a nondecaying Ca_i response was generated upon restoration of extracellular Ca^{2+} to the cells at a time after which the PAF-induced transient would have been expected to have fully decayed. These results would suggest that the opening of plasma membrane channels activated as a result of PAF receptor activation is independent of extracellular Ca^{2+}, and further, that channels opened in response to PAF remain open until such time that Ca^{2+} is restored. Alternatively, this pathway could represent a separate Ca^{2+} entry pathway related to store depletion similar to that described by Hoth and Penner (1992) in mast cells. However, restoration of Ca^{2+} to the external solution in Ca^{2+}-depleted cells in the absence of PAF stimulation

did not result in the generation of a Ca_i transient, indicating that channel opening is coupled to receptor ligation.

Dependence of PAF-Induced Ca_i Transient on Sodium-Calcium Exchange

Data reported in this study provide direct evidence for the importance of Na-Ca exchanger activity in the regulation of Ca_i. The observation that basal Ca_i in HMDMs was approximately doubled after removal of extracellular Na^+ indicates the presence of the antiporter in unstimulated cells and the involvement of Na-Ca exchange in the maintenance of Ca_i even at rest. Although removal of extracellular Na^+ increased basal Ca_i, it did not alter the magnitude or time course of the decay of the PAF-induced Ca^{2+} transient, which argues that PAF is not acting through the modulation of Na-Ca antiporter exchange. Similar results were obtained by Randriamampita and Trautmann (1990) in murine peritoneal macrophages. This suggests the existence of alternate high capacity Ca^{2+} buffering processes in the HMDM, whose activity may be enhanced following PAF stimulation. These include the Ca^{2+}-ATPase, cytoplasmic Ca^{2+} binding proteins, and intracellular organelles. Changes in the activity of the plasma membrane Ca^{2+}-ATPase have been shown to account for the rapid buffering of agonist-evoked Ca_i transients in pancreatic acinar cells (Tepikin et al., 1992).

The Relationship between Calcium Influx and Mobilization from Internal Stores

The relative timing of the agonist-stimulated release of Ca^{2+} from internal stores and influx has been reported to vary according to cell type and agonist. In ADP-stimulated platelets loaded with Fura-2, Mn^{2+} or Ca^{2+} influx has been shown to precede the release of Ca^{2+} from internal stores (Sage et al., 1989). Studies on Fura-2 loaded neutrophils stimulated with f-met-leu-phe, PAF, or leukotriene B_4 (Meritt et al., 1989) have suggested that the release of internal Ca^{2+} and influx of Mn^{2+} occur simultaneously, although time course information in the agonist-evoked influx studies in neutrophils may be difficult to resolve in populations of cells monitored by spectrofluorimetry due to the heterogeneity in the time course of the Ca_i responses. In similar experiments on human glioblastoma cells stimulated by platelet-derived growth factor (PDGF), Mn^{2+}-induced quenching of Indo-1 fluorescence (Szöllösi et al., 1991) demonstrated that receptor-operated Ca^{2+} channel opening occurred 55 sec after the initial increase in Ca_i. In our studies the opening of the plasma membrane pathway in PAF-stimulated HMDMs, as monitored Ba^{2+}-enhanced Fura-2 fluorescence, occurred approximately 10–15 sec after the initial increase in Ca_i.

The lag time between intracellular Ca^{2+} release and influx pathway activation may represent the time during which mediators of channel activation e.g., inositol 1,3,4,5-tetrakisphosphate ($InsP_4$) are generated. Recent studies in endothelial cells have shown that $InsP_4$ activates a Ca^{2+}-channel which is Mn^{2+} permeable (Lückhoff & Clapham, 1992). The channel described in the endothelial cells appears to mediate receptor-operated Ca^{2+} entry in that it is activated by receptors coupled to endothelial inositol phosphate turnover and subsequent Ca^{2+} influx in intact cells. Ca^{2+} released during the mobilization phase and $InsP_4$ may interact cooperatively, as suggested from the studies of Lückhoff and Clapham (1992), to activate the receptor-operated calcium channel. This cooperative interaction may also contribute to the observed time delay in channel opening.

PAF-stimulation activated a current in HMDMs through which divalent cations could permeate. However, large changes in current amplitude were not detected upon removal of Ca^{2+} from the extracellular solution. This suggests that only a small amount of the PAF-activated current may be carried by Ca^{2+} ions. This observation is similar to that made by Matthews, Neher and Penner (1989*a*) for the rat peritoneal mast cell. Agonist stimulation in the mast cell activated a large conductance cation channel which allowed permeation of divalent cations. The agonist-stimulated cation channel activated with a delay, as did the PAF-activated nonselective current in our studies. Matthews et al. (1989*a*) also noted the activation of an $InsP_3$-induced Ca^{2+} influx in the same studies on the mast cell. The $InsP_3$-activated current was associated with whole-cell currents of 1–2 pA or less, which they suggested might be due to the activation of small conductance channels that are highly calcium selective, or that the influx may not be through a conductive pathway. Matthews et al. (1989*a*) observed that the nonselective pathway contributed to the agonist-induced influx but that it was not the primary source. Instead, their data was consistent with the hypothesis that the $InsP_3$-mediated Ca^{2+}-selective conductance accounted for the bulk of the agonist-induced Ca^{2+} influx. It is possible that most of the divalent current in the PAF-stimulated macrophage is through a highly selective divalent pathway similar to that described in the agonist-stimulated mast cell. This possibility

would be consistent with our inability to detect significant whole-cell current changes in PAF-stimulated cells expected to correlate with changes observed in Ca_i upon removal of Ca_o.

Calcium influx into endothelial cells has been shown to be hyperpolarization-driven. Ca^{2+}, mobilized during the initial rise in Ca_i in response to agonist-receptor binding, activates K^+ channels thereby inducing hyperpolarization which provides the driving force for transmembrane Ca^{2+} influx (Lückhoff & Busse, 1990). Activation of a Cl^- current following mast cell stimulation hyperpolarizes the membrane potential and provides a driving force for the entry of Ca^{2+} through agonist-activated pathways (Matthews, Neher & Penner, 1989*b*).

In summary, we observed a PAF-induced increase in Ca_i in HMDMs which was associated with an increase in inward current. Inward current activation was closely linked to the initial phase of the transient Ca_i increase and was voltage independent. In the absence of Na^+ and K^+, the agonist-stimulated current appeared to be permeant to large cation substitutes and was not decreased upon removal of Ca_o, indicating that the bulk of the Ca^{2+} influx which contributed to the Ca_i transient was not through the nonselective conductance and that it occurs either through a parallel pathway of low conductance channels that are highly Ca^{2+} selective or possibly not via ion channels. In that IP_3 receptors have been localized to the plasma membrane of cells in the immune system and appear to be responsible for Ca^{2+} entry associated with the proliferative response in lymphocytes (Khan et al., 1992) it is likely that they might also be associated with the Ca^{2+} entry step in agonist-stimulated HMDMs and may indeed be an IP_3-gated highly selective Ca^{2+} conductance associated with the sustained phase of the integrated PAF-induced Ca_i transient in the macrophage.

References

Braquet, P., Touqil, L., Shen, T.Y., Vargaftig, B.B. 1987. Perspectives in platelet-activating factor research. *Pharmacol. Rev.* **39:**97–118

Conrad, G.W., Rink T.J. 1986. Platelet activating factor raises intracellular calcium ion concentration in macrophages. *J. Cell Biol.* **103:**439–450

Di Virgilio, F., Lew, P.D., Andersson, T., Pozzan, T. 1988. Plasma membrane potential modulates chemotactic peptide-stimulated cytosolic free Ca^{2+} changes in human neutrophils. *J. Biol. Chem.* **262:**4574–4579

Dixon, R.A.F., Kobilka, B.K., Strader, D.J., Benovic, J.L., Dohlman, H.G., Frielle, T., Bolanowski, M. A., Bennett, C.D., Rands, E., Diehl, R.E., Mumford, R.A., Slater, E.E., Sigal, I.S., Caron, M.G., Lefkowitz, R.J., Strader, C.D. 1986. Cloning of the gene and cDNA for mammalian β-adrenergic receptor and homology with rhodopsin. *Nature* **321:**75–79

Gerard, N.P., Gerard, C. 1991. The chemotactic receptor human C5a anaphylatoxin. *Nature* **349:**614–617

Grynkiewicz, G., Poenie, M., Tsien, R.Y. 1985. A new generation of Ca^{2+} indicators with greatly improved fluorescence properties. *J. Biol. Chem.* **260:**3440–3450

Hallam, T.J., Jacob, R., Merritt, J.E. 1988. Evidence that agonists stimulate bivalent cation influx into human endothelial cells. *Biochem. J.* **255:**179–184

Hallam, T.J., Rink, T.J. 1985. Agonists stimulate divalent cation channels in the plasma membrane of human platelets. *FEBS Lett.* **186:**175–179

Hara, N., Ichinose, M., Sawada, M., Maeno, T. 1991. The activation of Ca^{2+}-dependent K^+ conductance by adrenaline in mouse peritoneal macrophages. *Pfluegers Arch.* **419:**371–379

Hirata, M., Hayashi, Y., Ushikubi, F., Yokata, Y., Kageyama, R., Nakanishi, S., Narumiya S. 1991. Cloning and expression of cDNA for a human thromboxane A_2 receptor. *Nature* **349:**617–620

Honda, Z.I., Nakamura, M., Miki, I., Minami, M., Wantanabe, T., Seyama, Y., Okado, H., Toh, H., Ito, K., Miyamoto, T., Shimizu T. 1991. Cloning by functional expression of platelet-activating factor receptor from guinea-pig lung. *Nature* **349:**342–346

Hoth, M., Penner, R. 1992. Depletion of intracellular calcium stores activates a calcium current in mast cells. *Nature* **355:**353–355

Jacob, R. 1990. Agonist-stimulated divalent cation entry into single cultured human umbilical vein endothelial cells. *J. Physiol.***421:**55–77

Kass, G.E.N., Liopis, J., Chow, S.C., Duddy, S.K., Orrenius, S. 1990. Receptor-operated calcium influx in rat hepatocytes. *J. Biol. Chem.* **265:**17486–17492

Khan, A.A., Steiner, J.P., Klein, M.G., Schneider, M.F., Snyder, S.H. 1992. IP_3 Receptor: Localization to plasma membrane of T cells and cocapping with the T cell receptor. *Science* **257:**815–818

Kwan, C.-Y., Putney, J.W. 1990. Uptake and intracellular sequestration of divalent cations in resting and methacholine-stimulated mouse lacrimal acinar cells: Dissociation by Sr^{2+} and Ba^{2+} of agonist-stimulated divalent cation entry from the refilling of the agonist-sensitive intracellular pool. *J. Biol. Chem.* **265:**678–684

Lipton, S.A. 1986. Antibody activates cationic channels via second messenger Ca^{2+}. *Biochim. Biophys. Acta* **856:**59–67

Lückhoff, A., Busse, R. 1990. Calcium influx into endothelial cells and formation of endothelium-derived relaxing factor is controlled by the membrane potential. *Pfluegers Arch.* **416:**305–311

Lückhoff, A., Clapham D.E. 1992. Inositol 1,3,4,5-tetrakisphosphate activates an endothelial Ca^{2+}-permeable channel. *Nature* **355:**356–358

Malgaroli, A., Milani, D., Meldolesi, J., Pozzan, T. 1987. Fura-2 measurement of cytosolic free Ca^{2+} in monolayers and suspensions of various types of animal cells. *J. Cell Biol.* **105:**2145–2155

Matthews, G., Neher, E., Penner, R. 1989*a*. Second messenger-activated calcium influx in rat peritoneal mast cells. *J. Physiol.* **418:**105–130

Matthews, G., Neher, E., Penner, R. 1989*b*. Chloride conductance activated by external agonists and internal messengers in rat peritoneal mast cells. *J. Physiol.* **418:**131–144

Maudsley, D.J., Morris, A.G. 1987. Rapid intracellular calcium changes in U937 monocyte cell line: transient increases in response to platelet-activating factor and chemotactic peptide but not interferon-γ or lipopolysaccharide. *Immunology* **61:**189–194

Merritt, J.E., Jacob, R., Hallam, T.J. 1989. Use of manganese to discriminate between calcium influx and mobilization from internal stores in stimulated human neutrophils. *J. Biol. Chem.* **264:**1522–1527

Murray, R.K., Kotlikoff, M.I. 1991. Receptor-activated calcium influx in human airway smooth muscle cells. *J. Physiol.* **435:**123–144

Nelson, D.J., Jow, B., Jow, F. 1990. Whole-cell currents in macrophages I. Human monocyte derived macrophages. *J. Membrane Biol.* **117:**29–44

Ng, D.S., Wong, K. 1989. Effects of platelet-activating factor (PAF) on cytosolic free calcium in human peripheral blood mononuclear leukocytes. *Res. Comm. Chem. Path. and Pharm.* **64:**351–354

Ozaki, Y., Yatomi, Y., Kume, S. 1992. Evaluation of platelet calcium ion mobilization by the use of various divalent ions. *Cell Calcium* **13:**19–27

Prpic, V., Uhing, R.J., Weiel, J.E., Jakoi, L., Gawdi, G., Herman, B., Adams, D.O. 1988. Biochemical and functional responses stimulated by platelet-activating factor inmurine peritoneal macrophages. *J. Cell Biol.* **107:**363–372

Randriamampita, C., Trautmann, A. 1989. Biphasic increase in intracellular calcium induced by platelet-activating factor in macrophages. *FEBS Lett.* **249:**199–206

Randriamampita, C., Trautmann, A. 1990. Arachidonic acid activates Ca^{2+}extrusion in macrophages. *J. Biol. Chem.* **265:**18059–18062

Randriamampita, C., Bismuth, G., Trautmann, A. 1991. Ca^{2+}-induced Ca^{2+} release amplifies the Ca^{2+} response elicited by inositol trisphosphate in macrophages. *Cell Regul.* **2:**513–522

Sage, S.O., Merritt, J.E., Hallam, T.J., Rink, T.J. 1989. Receptor-mediated calcium entry in fura-2-loaded human platelets stimulated with ADP and thrombin. *Biochem. J.***258:**923–926

Steinberg, T.H., Newman, A. S., Swanson, J.A. 1987. Macrophages possess probenecid-inhibitable organic anion transporters that remove fluorescent dyes from the cytoplasmic matrix. *J. Cell Biol.* **105:**2695–2702

Szöllösi, J., Feuerstein, B.G., Vereb, G., Pershadsingh, H.A., Marton, L.J. 1991. Calcium channels in PDGF-stimulated A172 cells open after intracellular calcium release and are not voltage-dependent. *Cell Calcium* **12:**477–491

Tepikin, A.V., Voronina, S.G., Gallacher, D.V., Petersen, O.H. 1992. Acetylcholine-evoked increase in the cytoplasmic Ca^{2+} concentration and Ca^{2+} extrusion measured simultaneously in single mouse pancreatic acinar cells

Uhring, R.J., Prpic, V., Hollenbach, P.W., Adams, D.O. 1989. Involvement of protein kinase C in platelet-activating factor-stimulated diacylglycerol accumulation in murine peritoneal macrophages. *J. Biol. Chem.* **264:**9224–9230

Wood, D.A., Hapak, L.K., Sims, S.M., Dixon, S.J. 1991. Direct effects of platelet-activating factor on isolated rat osteoclasts. *J. Biol. Chem.***266:**15369–15376